Journal of Mahani Mathematical Research
Shahid Bahonar University of Kerman
Print ISSN: 2251-7952 Online ISSN: 2645-4505

NUMERICAL SOLUTIONS FOR FRACTIONAL OPTIMAL CONTROL PROBLEMS USING MÜNTZ-LEGENDRE POLYNOMIALS

M. Sahabi and A. Yazdani Cherati ✉

Article type: Research Article

(Received: 12 January 2024, Received in revised form 24 July 2024)

(Accepted: 18 August 2024, Published Online: 04 September 2024)

Abstract. This study introduces a novel method using the Müntz-Legendre polynomials for numerically solving fractional optimal control problems. Utilizing the unique properties of Müntz-Legendre polynomials when dealing with fractional operators, these polynomials are used to approximate the state and control variables in the considered problems. Consequently, the fractional optimal control problem is transformed into a nonlinear programming problem through collocation points, yielding unknown coefficients. To achieve this, stable and efficient methods for calculating the fractional integral and derivative operators of Müntz-Legendre functions based on three-term recurrence formulas and Jacobi-Gauss quadrature rules are presented. A thorough convergence analysis, along with error estimates, is provided. Several numerical examples are included to demonstrate the efficiency and accuracy of the proposed method.

Keywords: Müntz-Legendre Polynomials, Fractional Optimal Control Problems, Convergence analysis, Numerical techniques.
2020 MSC: Primary 26Cxx, 34H05, 49M05, 49M37, 65D05.

1. Introduction

Fractional-order dynamics appear in many areas of science and engineering, including fluid dynamics, space exploration, signal processing, robotics, and economics [6, 18, 34]. Recently, it has been shown that many systems can be better described using fractional differential equations (FDEs) rather than traditional integer differential equations (IDEs). For more details on fractional calculus, you can refer to sources such as [16, 17, 30]. Fractional Optimal Control Problems (FOCPs) are a type of optimal control problem. These problems aim to minimize a performance index within a feasible set of control and state variables, where the system dynamics are described by FDEs. Additional constraints, such as final time, can also be included in FOCPs. The dynamics in these problems can be described by different types of fractional derivatives, such as Riemann-Liouville fractional derivatives (RLFD) and Caputo fractional

✉ yazdani@umz.ac.ir, ORCID: 0000-0002-3352-5829
https://doi.org/10.22103/jmmr.2024.22811.1565

Publisher: Shahid Bahonar University of Kerman
How to cite: M. Sahabi, A. Yazdani Cherati, *Numerical solutions for fractional optimal control problems using Müntz-Legendre polynomials*, J. Mahani Math. Res. 2025; 14(1): 189-217.

derivatives (CFD).
Due to the wide range of applications of FOCPs, a lot of effort has been put into finding solutions, making it an important research area. Since analytical solutions are often difficult to obtain for most FOCPs, except in special cases, approximation methods are essential. In recent years, numerical methods have become the preferred approach for finding approximate solutions to FOCPs (see [10, 12, 15, 19, 25, 26, 33, 35]).
Generally, there are two main categories for addressing FOCPs: indirect and direct methods. In indirect methods, the necessary optimality conditions of FOCPs are determined using Pontryagin's minimum principle [3, 25]. In direct methods, a continuous FOCP is converted into a finite-dimensional nonlinear programming problem (NLP) by parameterizing the state and/or control variables [12,13,20,21,29,36]. In [32], a collocation method using Bessel functions is employed for the numerical solution of FOCPs. Among global direct methods, pseudospectral methods are very effective for solving FOCPs. These methods are widely used for solving optimal control problems, such as the Gauss pseudospectral and Radau pseudospectral methods [1, 2, 10, 29]. Moreover, in [10], a unified framework for solving FOCPs using integral pseudospectral methods has been provided, and [14] discusses optimal control problems with time delay in the calculus of variations.
The construction of derivative and integral matrices using classical polynomials, such as Jacobi polynomials, is a key feature of these methods. Given that problems with fractional operators often yield non-smooth solutions even when the input data is smooth, existing methods based on classical polynomials typically exhibit low convergence rates. Therefore, in this paper, we have chosen M*ü*ntz-Legendre polynomials to solve fractional optimal control problems, as they are better suited to fractional integral and derivative operators. The orthogonal M*ü*ntz systems were initially considered by Badalyan [4] and Taslakyan [31]. M*ü*ntz polynomials have a key feature: their fractional integrals and derivatives can be directly expressed in terms of the same polynomials. This sets M*ü*ntz polynomials apart from classical polynomials, which do not have polynomial forms for their fractional operators. Because of this important feature, M*ü*ntz-Legendre polynomials have been used in various papers to find numerical solutions for FDEs [8, 9, 23] and FOCPs [7].
kkkkk In recent years, M*ü*ntz-Legendre polynomials have been used to solve various equations involving fractional operators. However, most of these studies have not focused on the specific computation of the fractional operators of these polynomials. Instead, they use the explicit forms of M*ü*ntz-Legendre polynomials to obtain operational matrices for fractional integration and differentiation. These approaches often lead to instability when constructing the operational matrices, making the method unsuitable as the number of basis functions increases. In this work, we address this issue by developing a method specifically for solving fractional optimal control problems, ensuring stability

and accuracy even as the number of basis functions increases. Next, we briefly highlight the main contributions of our development:

- We have developed an effective and stable method for computing fractional integral and derivative operators of Müntz-Legendre functions.
- We have created an efficient numerical method for solving nonlinear fractional optimal control problems by transforming the given problem into a nonlinear programming problem.
- We have conducted a convergence analysis and provided error estimates for the proposed method.
- The method is designed for practical implementation, demonstrating its robustness and effectiveness in real-world complex problems.

The subsequent sections of this paper are organized as follows: Section 2 provides a brief overview and some basic definitions and preliminaries of fractional calculus, fractional optimal control problems (FOCPs), and Müntz-Legendre polynomials. New methods for evaluating fractional operators of Müntz-Legendre polynomials are presented in Section 3. Section 4 applies a new method to solve FOCPs, and in Section 5, we compute error bounds for fractional operators and dynamic systems. Several examples are given to demonstrate the accuracy of the proposed methods in Section 6. The conclusions are discussed in the final section.

2. Mathematical Preliminaries

2.1. **Fractional Calculus.** In this section we present some basic definitions needed in the following parts of the paper. For more detailed information, interested readers can refer to [17,25].

Definition 2.1. Let $f : [a,b] \longrightarrow \mathbb{R}$ be a function and $\alpha > 0$ be a real number. The RLFI of a function $f(t)$ are defined as [17]:

$$_aI_t^\alpha f(t) = \frac{1}{\Gamma(\alpha)} \int_a^t (t-s)^{\alpha-1} f(s) ds, \quad t > a,$$

and CFD are given according to

$$^c_aD_t^\alpha f(t) = \frac{1}{\Gamma(n-\alpha)} \int_a^t (t-s)^{n-\alpha-1} f^{(n)}(s) ds, \quad t > a,$$

where $n = [\alpha] + 1$ and $\Gamma(.)$ is gamma function.

We discuss the different characteristics of fractional integrals and derivatives, highlighting a few of them [17]. As evident below, applying the RLFI and CFD operators to power functions results in power functions of the same form. Assuming $\alpha > 0$ and $\beta > -1$, the following identities hold

$$_aI_t^\alpha (t-a)^\beta = \frac{\Gamma(\beta+1)}{\Gamma(\beta+\alpha+1)} (t-a)^{\beta+\alpha}, \tag{1}$$

and

$$
{}_a^c D_t^\alpha (t-a)^\beta = \begin{cases} 0, & \alpha = 0,1,\ldots,n-1, \\ \frac{\Gamma(\alpha+1)}{\Gamma(\beta-\alpha+1)}(t-a)^{\beta-\alpha}, & \beta > n-1. \end{cases} \tag{2}
$$

Moreover, If $f(t) \in \mathbb{C}^n[a,b]$ the fractional integrals and derivatives have the following properties [24]

$$
{}_a I_t^\alpha ({}_a^c D_t^\alpha) f(t) = f(t) - \sum_{k=0}^{n-1} \frac{f^{(k)}(a)}{k!}(t-a)^k, \tag{3}
$$

and

$$
{}_a I_t^{\alpha-\beta} ({}_a^c D_t^\alpha) f(t) = {}_a^c D_t^\alpha f(t), \qquad \alpha > \beta > 0. \tag{4}
$$

2.2. **Fractional Optimal Control Problems.** In this paper, we suppose that $n-1 < \alpha < n$ be a real number, $\Omega = [0,T]$, and the state and control variable $x, u : \Omega \longrightarrow \mathbb{R}$, let $F, G : [0,\infty) \times \mathbb{R}^2 \longrightarrow \mathbb{R}$ are continuously differentiable, the general form of FOCPs can be introduced as minimize the cost functional

$$
J = \phi(T, x(T)) + \int_0^T F(t, x(t), u(t)) dt, \qquad t \in [0,T], \tag{5}
$$

subject to the system dynamics

$$
A x^{(n)}(t) + B\, {}_0^c D_t^\alpha x(t) = G(t, x(t), u(t)), \tag{6}
$$

(7)

with $A, B \neq 0$ and the initial condition $x(0) = x_0$. Also $\phi(t, x(t))$ is called the final function.

2.3. **The M$\ddot{u}$ntz -Legendre Polynomials.** Let the complex sequence $\Lambda = \{\lambda_0, \lambda_1, \ldots\}$ be such that $Re(\lambda_i) > -1/2$ for every $i = 0, 1, \ldots$. The M$\ddot{u}$ntz polynomials can be expressed on the interval $(0,1]$ in power form as (see [5,22])

$$
P_k(t) := P_k(t; \Lambda_k) = \sum_{i=0}^{k} C_{k,i} t^{\lambda_i}, \qquad C_{k,i} = \frac{\prod_{j=0}^{k-1}(\lambda_i + \bar{\lambda}_j + 1)}{\prod_{j=0, j\neq i}^{k}(\lambda_i - \lambda_j)}. \tag{8}
$$

In this paper, the case $\lambda_i = i\alpha$ is considered and then the M$\ddot{u}$ntz -Legendre polynomials on the interval $[0,T]$ are represented by the formula

$$
L_k(t;\alpha) = \sum_{i=0}^{k} C_{k,i} (\frac{t}{T})^{i\alpha}, \quad C_{k,i} = \frac{(-1)^{k-i}}{\alpha^k i!(k-i)!} \prod_{j=0}^{k-1}((i+j)\alpha + 1). \tag{9}
$$

It can be shown that

$$\int_0^T L_k(t)L_i(t)dt = \frac{T}{2k\alpha+1}\delta_{ki}.$$

We denote the corresponding M*ü*ntz- Legendre by $\mathbb{M} = \bigcup_{n=0}^{\infty} M_{n,\alpha}$, where $M_{n,\alpha}$ is defined by

$$M_{n,\alpha} = span\left\{1, t^{\alpha}, ..., t^{n\alpha}\right\}, = \left\{\sum_{k=0}^{n} c_k t^{k\alpha} : c_k \in \mathbb{R}\right\}, \quad t \in [0,T].$$

It can be shown that the M*ü*ntz- Legendre polynomials of the form $\sum_{k=0}^{n} c_k t^{k\alpha}$ with real coefficients are completeness and dense in $L^2(0,1)$ [5, 22]. Now, the function f(t) which belong to $L^2(0,T)$, may be expressed in terms of M*ü*ntz-Legendre polynomials as

$$f(t) = \sum_{i=0}^{\infty} f_i L_i(t;\alpha)$$

where the coefficients are given by

$$f_i = (2i\alpha+1)\int_0^T f(t)L_i(t;\alpha)dt, \quad i = 0,1,2,\dots \tag{10}$$

Due to the substantial increase in the coefficients $C_{n,k}$ with growing n, the direct evaluation of M*ü*ntz-Legendre polynomials using the power form (9) can pose challenges, as highlighted in [22]. The explicit form (9) becomes increasingly unstable and deficient, particularly for larger values of n. For

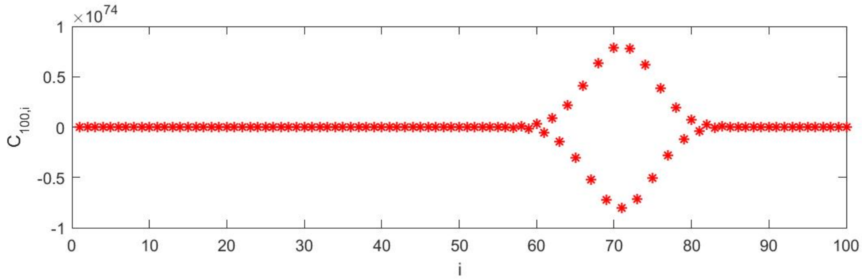

FIGURE 1. The coefficients of M*ü*ntz- Legendre polynomials for $L_{100}(t; \frac{1}{2})$.

example, in Fig. 1, for $n = 100$ and $\alpha = \frac{1}{2}$, we can see how the coefficients of the M*ü*untz-Legendre polynomials ($C_{100,k}$) increase very quickly. Therefore, we cannot use the form (9) in practical problems such as FDEs and FOCPs that require a large n for approximating their solutions. In the paper [9], an efficient technique based on a three-term recurrence relation is proposed, which is derived from the following.

$$L_k(t;\alpha) = P_k^{0,\frac{1}{\alpha}-1}(2(\frac{t}{T})^\alpha - 1), \quad k = 0, 1, \ldots, \tag{11}$$

where $P_n^{\alpha,\beta}(t)$ with parameters $\alpha, \beta > -1$ are well known Jacobi polynomials defined on the interval $[-1, 1]$. An immediate consequence is the recurrence relation of Müntz-Legendre polynomials, we have

(12)

$$\begin{array}{l} L_0(t;\alpha) = 1, \qquad L_1(t;\alpha) = (\frac{1}{\alpha}+1)(\frac{t}{T})^\alpha - \frac{1}{\alpha}, \\ L_{k+1}(t;\alpha) = (a_k(2(\frac{t}{T})^\alpha - 1) - b_k)L_k(t;\alpha) - c_k L_{k-1}(t;\alpha), \quad k = 1, 2, \ldots, \end{array}$$

where

$$a_k = \frac{(2k+\frac{1}{\alpha})(2k+\frac{1}{\alpha}+1)}{2(k+1)(k+\frac{1}{\alpha})}, \quad b_k = \frac{(2k+\frac{1}{\alpha})(\frac{1}{\alpha}-1)^2}{2(k+1)(k+\frac{1}{\alpha})(2k+\frac{1}{\alpha}-1)},$$
$$c_k = \frac{k(2k+\frac{1}{\alpha})(k+\frac{1}{\alpha}-1)}{(k+1)(k+\frac{1}{\alpha})(2k+\frac{1}{\alpha}-1)}.$$

The stability and efficiency of the recurrence formulas are demonstrated in

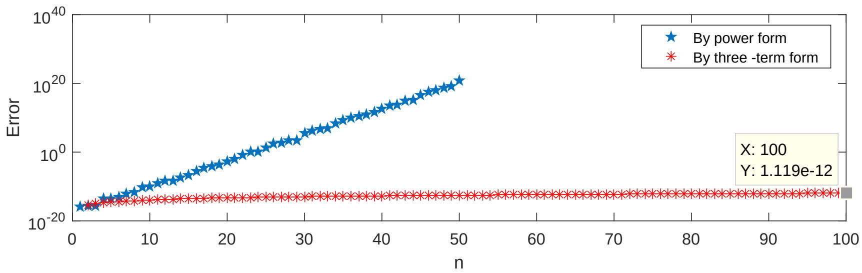

FIGURE 2. Absolute error for the approximation of $L_n(t, \frac{1}{2})$ for $t = 1$ and $t = 1 - 10^{-16}$.

Fig. 2, where the absolute error of $L_n(t, 1/2)$ is plotted for $t = 1$ and $t = 1 - \varepsilon$ ($\varepsilon = 10^{-16}$) for $n = 1, 2, \ldots, 100$. Nevertheless, we can obtain

$$\mid L_n(1, \frac{1}{2}) - L_n(1-\varepsilon, \frac{1}{2}) \mid \approx |\varepsilon L_n'(1, \frac{1}{2})| = \varepsilon \frac{n(n+2)}{2},$$

3. Numerical Evaluation of Fractional Operators of $L_n(t;\alpha)$

If $L_k(t;\alpha)$ is defined by (9), then the RLFI and CFD of $L_k(t;\alpha)$ for $k = 0, 1, \ldots$ according to (1) can be expressed in the following forms:

$$\begin{array}{ll} {}_0I_t^\alpha L_k(t;\alpha) = \sum_{i=0}^k D_{k,i}^1 (\frac{t}{T})^{(i+1)\alpha}, & D_{k,i}^1 = \frac{\Gamma(1+i\alpha)}{\Gamma(1+(i+1)\alpha)} C_{k,i}, \\ {}_0^cD_t^\alpha L_k(t;\alpha) = \sum_{i=1}^k D_{k,i}^2 (\frac{t}{T})^{(i-1)\alpha}, & D_{k,i}^2 = \frac{\Gamma(1+i\alpha)}{\Gamma(1+(i-1)\alpha)} C_{k,i}. \end{array} \tag{13}$$

Also, according to (1), we should have ${}_0D_t^\alpha L_k(t;\alpha) = {}_0^cD_t^\alpha L_k(t;\alpha)$, and ${}_0^cD_t^\alpha L_k(t;\alpha) \in M_{k-1,\alpha}$ and ${}_0I_t^\alpha L_k(t;\alpha) \in M_{k+1,\alpha}$.
Once again, we observe that the coefficients D^1k, i and D^2k, i become very large with increasing n, and direct evaluation of fractional operators of $L_k(t,\alpha)$ can encounter issues. In this section, we propose stable numerical methods for evaluating the values of fractional operators of Müntz-Legendre polynomials, which are essential for solving FOCPs in the subsequent sections. In [9], a numerical method is introduced for evaluating ${}_0^cD^\alpha t L_k(t;\alpha)$

Theorem 3.1. *Let $0 < \alpha < 1$ be a real number and $t \in [0,T]$. Then the representation*

$$\begin{aligned} {}_0^cD_t^\alpha L_k(t;\alpha) &= \tfrac{1+k\alpha}{\alpha\Gamma(1-\alpha)T^\alpha}\int_0^1 (1-x^{\frac{1}{\alpha}})^{-\alpha} P_{k-1}^{1,\frac{1}{\alpha}}(2(\tfrac{t}{T})^\alpha x - 1)dx \\ &= \tfrac{1+k\alpha}{\alpha\Gamma(1-\alpha)T^\alpha}\textstyle\sum_{i=1}^{\lceil \frac{k}{2}\rceil} \omega_{i,\alpha} P_{k-1}^{1,\frac{1}{\alpha}}(2(\tfrac{t}{T})^\alpha \tau_{i,\alpha} - 1), \end{aligned} \tag{14}$$

holds true.

The weight function $w(x;\alpha) = (1-x^{\frac{1}{\alpha}})^{-\alpha}$ remains nonclassical, and there are no explicit formulas for calculating nodes and weights to evaluate (14). A technique employing the Chebyshev algorithm is provided for obtaining nodes $\tau_{i,\alpha}$ and weights $\omega_{i,\alpha}$. Nevertheless, this algorithm is generally acknowledged for its numerical instability. In numerous instances, the modified Chebyshev algorithm has been introduced as an alternative to stabilize the computation. However, it's worth noting that the tendency to become ill-conditioned poses a limitation [11], particularly for larger k (see Fig. 3). In order to improve that, Let $x = z^\alpha$ and using [**?**]

$$P_{k-1}^{1,\frac{1}{\alpha}}(2(\frac{t}{T})^\alpha - 1) = \sum_{j=0}^{k-1} \hat{c}_{k-1,j} L_k(t;\alpha) = \hat{\mathbf{C}}_k \mathbb{L}_k(t;\alpha),$$

where $\hat{c}_{k-1,j}$ is obtained as

$$\hat{c}_{k-1,j} = \frac{k!(2j+\frac{1}{\alpha})\Gamma(j+\frac{1}{\alpha})}{j!\Gamma(k+\frac{1}{\alpha}+1)} \sum_{m=0}^{k-j-1} (-1)^m \frac{\Gamma(k+j+m+\frac{1}{\alpha}+1)}{m!(k-j-m-1)!(m+j+1)\Gamma(m+2j+\frac{1}{\alpha}+1)}.$$

Then we can obtain

$$\begin{aligned} {}_0^cD_t^\alpha L_k(t;\alpha) &= \tfrac{1+k\alpha}{\Gamma(1-\alpha)T^\alpha}\int_{-1}^1 w^{-\alpha,\alpha-1}(z) P_{k-1}^{1,\frac{1}{\alpha}}(2(\tfrac{z+1}{2T}t)^\alpha - 1)dz, \\ &= \tfrac{1+k\alpha}{\Gamma(1-\alpha)T^\alpha}\textstyle\sum_{j=1}^{\lceil \frac{k}{2}\rceil} \omega_j^\alpha P_{k-1}^{1,\frac{1}{\alpha}}(2(\tfrac{\tau_j^\alpha+1}{2T}t)^\alpha - 1) \\ &= \tfrac{1+k\alpha}{\Gamma(1-\alpha)T^\alpha}\hat{\mathbf{C}}_k \textstyle\sum_{j=1}^{\lceil \frac{k}{2}\rceil} \omega_j^\alpha \mathbb{L}_k(t\tfrac{\tau_j^\alpha+1}{2};\alpha), \end{aligned} \tag{15}$$

where $w^{-\alpha,\alpha-1}(z) = (1-z)^{-\alpha}(1+z)^{\alpha-1}$ represents a Jacobi weight function over $(-1,1)$, and ω_j^α and τ_j^α are Jacobi-Gauss-type nodes and their corresponding weights, the formula loses its utility with increasing k. As the coefficients $\hat{c}_{k-1,i}$ become very large (distinct from the growth of $D^2_{k,i}$), achieving precise evaluations of ${}_0^cD_t^\alpha L_k(t_i;\alpha)$ for large k becomes challenging. It's noteworthy that this formula maintains better stability compared to (13) and (14) (see Fig. 3). Similarly, we can evaluate ${}_0I_t^\alpha L_k(t;\alpha)$ using the following expression:

$$\begin{aligned}{}_0I_t^\alpha L_k(t;\alpha) &= \frac{1}{\Gamma(\alpha)}(\frac{t}{2})^\alpha \int_{-1}^{1} w^{0,\alpha-1}(z) L_k(t\frac{z+1}{2};\alpha)dz \\ &= \frac{1}{\Gamma(\alpha)}(\frac{t}{2})^\alpha \sum_{j=1}^{\lceil \frac{k}{2} \rceil} \hat{\omega}_j^\alpha L_k(t\frac{\hat{\tau}_j^\alpha+1}{2};\alpha),\end{aligned}$$

where $\hat{\tau}_j^\alpha$ and $\hat{\omega}_j^\alpha$ are nodes and weights corresponding $w^{0,\alpha-1}(z)$.
In the subsequent sections, we introduce an alternative approach for assessing RLFI and CFD, which proves to be more suitable and significantly stable. This is achieved by employing a three-term recurrence relation (12). We have ${}_a^cD_t^\alpha t^\alpha L_k(t;\alpha) \in \mathbf{M}_{k,\alpha}$ then

$${}_a^cD_t^\alpha t^\alpha L_k(t;\alpha) = \sum_{i=0}^{k} \frac{\Gamma(1+(i+1)\alpha)}{\Gamma(1+i\alpha)} C_{k,i} t^{i\alpha} = \sum_{i=0}^{k} D_{k,i}^3 t^{i\alpha},$$

we can obtain the coefficients $\xi_{k,j}$ $(j = 0, 1, \ldots, k)$ such as

$${}_0^cD_t^\alpha t^\alpha L_k(t;\alpha) = \sum_{j=0}^{k} \xi_{k,j} L_j(t;\alpha).$$

For computing $\xi_{k,j}$ we have the triangular system that it can be solved by $(k+1)$ recursive elimination steps of the form

$$\begin{aligned}\xi_{k,k} &= \frac{D_{k,k}^3}{C_{k,k}}, \\ \xi_{k,j} &= \frac{D_{k,j}^3 - \sum_{i=j+1}^{k} C_{i,j}\xi_{k,i}}{C_{j,j}}, \qquad j = k-1, k-2, \ldots, 0\end{aligned}$$

This algorithm requires $(k+1)^2$ flops and it is easy to check the $\xi_{k,j}$ are much smaller than $D_{k,j}^2$. Finally by using three- term recurrence (12), we can compute left CFD as follows

(16)
$$\begin{aligned}&{}_0^cD_t^\alpha L_0(t;\alpha) = 0, \qquad {}_0^cD_t^\alpha L_1(t;\alpha) = \tfrac{1}{T^\alpha}(1+\tfrac{1}{\alpha})\Gamma(1+\alpha), \\ &{}_0^cD_t^\alpha L_{k+1}(t;\alpha) = \tfrac{2a_k}{T^\alpha}({}_0^cD_t^\alpha t^\alpha L_k(t;\alpha)) - (a_k+b_k){}_0^cD_t^\alpha L_k(t;\alpha) - c_k\, {}_0^cD_t^\alpha L_{k-1}(t;\alpha) \\ &\qquad = \tfrac{2a_k}{T^\alpha}\textstyle\sum_{j=0}^{k} \xi_{k,j} L_j(t;\alpha) - (a_k+b_k){}_0^cD_t^\alpha L_k(t;\alpha) - c_k\, {}_0^cD_t^\alpha L_k(t;\alpha), \\ &\qquad\quad k = 1, 2, \ldots\end{aligned}$$

In below, we try to give a similar method to evaluate ${}_0I_t^\alpha L_k(t;\alpha)$. Since ${}_0I_t^\alpha t^\alpha L_k(t;\alpha) \in \mathbb{M}_{k+2,\alpha}$, so we can write

$${}_0I_t^\alpha t^\alpha L_k(t;\alpha) = t^{2\alpha} \sum_{i=0}^{k} \frac{\Gamma(1+(i+1)\alpha)}{\Gamma(1+(i+2)\alpha)} C_{k,i} t^{i\alpha} = t^{2\alpha} \sum_{i=0}^{k} D_{k,i}^4 t^{i\alpha} = t^{2\alpha} \sum_{j=0}^{k} \hat{\xi}_{k,j} L_j(t;\alpha),$$

where it can be possible that we compute $\hat{\xi}_j$ like ξ_j by replacing $D^4_{k,i}$ instead $D^3_{k,i}$. Now, by using three- term recurrence, for $k = 1, 2, \ldots$, we have

$$
{}_0I_t^{\alpha} L_0(t;\alpha) = \frac{1}{\Gamma(1+\alpha)} t^{\alpha}, \qquad {}_0I_t^{\alpha} L_1(t;\alpha) = \frac{1}{T^{\alpha}}(1+\frac{1}{\alpha})\frac{\Gamma(1+\alpha)}{\Gamma(1+2\alpha)} t^{2\alpha} - \frac{1}{\alpha\Gamma(1+\alpha)} t^{\alpha},
$$

$$
\begin{aligned}
{}_0I_t^{\alpha} L_{k+1}(t;\alpha) &= \frac{2a_k}{T^{\alpha}}({}_0I_t^{\alpha} t^{\alpha} L_k(t;\alpha)) - (a_k+b_k){}_0I_t^{\alpha} L_k(t;\alpha) - c_k\, {}_0I_t^{\alpha} L_{k-1}(t;\alpha) \\
&= \frac{2a_k}{T^{\alpha}} t^{2\alpha} \sum_{j=0}^{n} \hat{\xi}_{k,j} L_j(t;\alpha) - (a_k+b_k){}_0I_t^{\alpha} L_k(t;\alpha) - c_k\, {}_0I_t^{\alpha} L_{k-1}(t;\alpha).
\end{aligned}
$$

Here, we present a new efficient method for fractional operators of Müntz-Legendre polynomials.

$$
\begin{aligned}
{}_0^cD_t^{\alpha} t^{\alpha} L_k(t;\alpha) &= \frac{1}{\Gamma(1-\alpha)} \int_0^t (t-s)^{-\alpha} (s^{\alpha} L_k(s;\alpha))' ds \\
&= \tfrac{1}{\Gamma(1-\alpha)} \int_0^t (t-s)^{-\alpha} (\alpha s^{\alpha-1} L_k(s;\alpha) + s^{\alpha} L_k'(s;\alpha)) ds \\
&= \tfrac{\alpha}{\Gamma(1-\alpha)} \int_0^t t^{-\alpha}(1-\tfrac{s}{t})^{-\alpha} \tfrac{s^{\alpha-1}}{t^{\alpha-1}} t^{\alpha-1} L_k(s;\alpha) ds \\
&+ \tfrac{1}{\Gamma(1-\alpha)} \int_0^t t^{-\alpha}(1-\tfrac{s}{t})^{-\alpha} \tfrac{s^{\alpha-1}}{t^{\alpha-1}} t^{\alpha-1} s L_k'(s;\alpha) ds \\
&= \tfrac{\alpha E_k}{\Gamma(1-\alpha)} \int_0^1 (1-\theta)^{-\alpha} \theta^{\alpha-1} \mathbb{L}_k(t\theta;\alpha) d\theta \\
&+ \tfrac{A_k}{\Gamma(1-\alpha)} \int_0^1 (1-\theta)^{-\alpha} \theta^{\alpha-1} \mathbb{L}_k(t\theta;\alpha) d\theta \\
&= \tfrac{\alpha E_k + A_k}{\Gamma(1-\alpha)} \int_{-1}^1 w^{-\alpha,\alpha-1}(z) \mathbb{L}_k(t\tfrac{1+z}{2};\alpha) dz \\
&= \tfrac{\alpha E_k + A_k}{\Gamma(1-\alpha)} \sum_{j=1}^{\lceil \frac{k}{2} \rceil} \omega_j^{\alpha} \mathbb{L}_k(t\tfrac{1+\tau_j^{\alpha}}{2};\alpha),
\end{aligned}
\tag{17}
$$

where $s = t\theta$, $z = 2\theta - 1$, A_k and E_k kth row of matrix A and identity matrix, respectively. Also, for RLFI we can conclude the following result

$$
\begin{aligned}
{}_0I_t^{\alpha} t^{\alpha} L_k(t;\alpha) &= \frac{1}{\Gamma(\alpha)} (\frac{t}{2^{\alpha}})^2 \int_{-1}^1 w^{\alpha-1,\alpha}(z) L_k(t\frac{1+z}{2};\alpha) dz \\
&= \frac{1}{\Gamma(\alpha)} (\frac{t}{2^{\alpha}})^2 \sum_{j=1}^{\lceil \frac{k}{2} \rceil} \breve{\omega}_j^{\alpha} L_k(t\frac{1+\breve{\tau}_j^{\alpha}}{2};\alpha).
\end{aligned}
$$

Similarly to (16), employing a three-term recurrence, we can derive stable methods for evaluating RLFI and CFD. These methods will be instrumental in solving FOCPs, as discussed in the subsequent section. Additionally, to compute the values of $L^{(m)}(t;\alpha)$ for $t \in (0, T]$, we can express it as follows:

$$
L_0^{(m)}(t;\alpha) = 0, \qquad L_1^{(m)}(t;\alpha) = \frac{\alpha+1}{T^{\alpha}}(\alpha-1)(\alpha-2)\ldots(\alpha-m+1)t^{\alpha-m},
$$

$$
\begin{aligned}
L_{k+1}^{(m)}(t;\alpha) &= \frac{2a_k}{T^{\alpha}}(\sum_{i=0}^{m} \begin{pmatrix} n \\ i \end{pmatrix} \alpha(\alpha-1)(\alpha-2)\ldots(\alpha-i+1)t^{\alpha-i} L_k^{(m-i)}(t;\alpha)) \\
&- (a_k+b_k) L_k^{(m)}(t;\alpha) - c_k L_{k-1}^{(m)}(t;\alpha), \qquad k, m = 1, 2, \ldots
\end{aligned}
$$

It is easy to generalize these results to the general case $n-1 < \alpha < n$. In Fig.

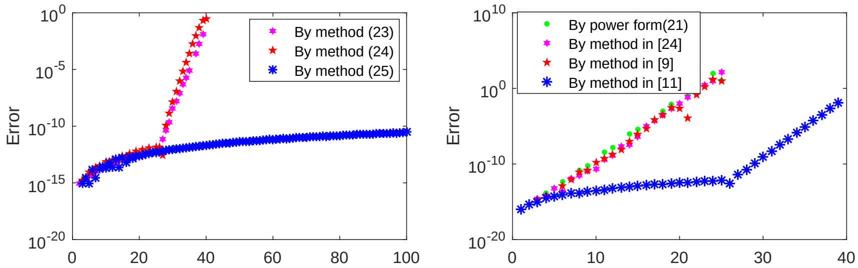

FIGURE 3. Absolute error for the approximation of ${}_0^cD_t^\alpha L_n(t,\frac{1}{2})$ for $t=1$ and $t=1-10^{-16}$ obtained from different methods.

3 (left), the absolute error for ${}_0^cD_t^\alpha L_k(t;\frac{1}{2})$ when $t=1,1-\varepsilon$ computed using three methods (15), (16) and (17) are demonstrated. Also at right, we show the error for 4 methods that are introduced in [7,9,23] and power form (13).

4. Numerical Method For Solving FOCPs

In this subsection, we propose a new strategy based on the Müntz- Legendre polynomials for solving FOCPs. In this way, we consider the following FOCPs

(18)

$$\begin{aligned} &J=\phi(T,x(T))+\int_0^T f(t,x(t),u(t))dt, \qquad t\in[0,T],\\ &\quad s.t \qquad Ax^{(k)}(t)+B\,{}_0^cD_t^\alpha x(t)=g(t,x(t))+a(t)u(t), \quad k<\alpha<k+1, \quad k=0,1,\ldots\\ &\qquad\qquad x^{(i)}=x_i, \qquad i=0,1,\ldots,k \end{aligned}$$

By the Müntz- Legendre basis, we approximate $y(t):={}_0^cD_t^\alpha x(t)$ as

$$y(t)\approx y_n(t)=\sum_{j=0}^n y_jL_j(t;\alpha), \tag{19}$$

where

$$y_j=(2j\alpha+1)\int_0^T L_j(t;\alpha)\,{}_0^cD_t^\alpha x(t)dt.$$

Now, by taking $\beta=k$ in (4) and using (3), we represent the $x(t)$ and $x^{(k)}(t)$ in the forms

$$\begin{aligned} x(t)&={}_0I_t^\alpha\,{}_0^cD_t^\alpha x(t)+\textstyle\sum_{i=0}^k\frac{x_i}{i!}t^i={}_0I_t^\alpha y(t)+\sum_{i=0}^k\frac{x_i}{i!}t^i,\\ x^{(k)}(t)&={}_0^cD_t^k x(t)={}_0I_t^{\alpha-k}\,{}_0^cD_t^\alpha x(t)={}_0I_t^{\alpha-k}y(t). \end{aligned} \tag{20}$$

We compute the control function $u(t)$ from the system dynamic and use (19) and (20)

(21)
$$u(t) = \frac{1}{a(t)}(Ax^{(k)}(t) + B\, {}_0^cD_t^\alpha x(t) - g(t, x(t)) \\ = \frac{1}{a(t)}(A\, {}_0I_t^{\alpha-k}y(t) + By(t) - g(t, {}_0I_t^\alpha y(t) + \textstyle\sum_{i=0}^k \frac{x_i}{i!}t^i)).$$

Utilizing (20) and (21), we can determine the approximation of $x(t)$, $x^{(k)}(t)$ and $u(t)$ as follows

$$x(t) \approx x_n(t) = {}_0I_t^\alpha y_n(t) + \sum_{i=0}^k \frac{x_i}{i!}t^i = \sum_{j=0}^n y_j\, {}_0I_t^\alpha L_j(t;\alpha) + \sum_{i=0}^k \frac{x_i}{i!}t^i,$$

$$u(t) \approx u_n(t) = \frac{1}{a(t)}(A\sum_{j=0}^n y_j\, {}_0I_t^{\alpha-k}L_j(t;\alpha) + B\sum_{j=0}^n y_j L_j(t;\alpha) - g(t, \sum_{j=0}^n y_j\, {}_0I_t^\alpha L_j(t;\alpha) + \sum_{i=0}^k \frac{x_i}{i!}t^i),$$

$$x^{(k)}(t) \approx x_n^{(k)}(t) = \sum_{j=0}^n y_j\, {}_0I_t^{\alpha-k}L_j(t;\alpha),$$

and substituting (20) and (21) into the performance index J gives

$$J = \phi(T, {}_0I_T^\alpha y(t) + \sum_{i=0}^k \frac{x_i}{i!}T^i) + \int_0^T f(t, {}_0I_t^\alpha y(t) \\ + \sum_{i=0}^k \frac{x_i}{i!}t^i, \frac{1}{a(t)}(A\, {}_0I_t^{\alpha-k}y(t) + By(t) - g(t, {}_0I_t^\alpha y(t) + \sum_{i=0}^k \frac{x_i}{i!}t^i))dt.$$

So, by using the above approximations and the Legendre -Gauss quadrature, the performance index can be approximated by $n+1$ variables y_j, $j = 0, 1, \ldots, n$

as follow

$$\begin{aligned}
J_n(y_0,y_1,\dots,y_n) &= \phi(T,\sum_{j=0}^{n} y_j\ {}_0I_T^{\alpha}L_j(t;\alpha)+\sum_{i=0}^{k}\frac{x_i}{i!}T^i)\\
&+\int_0^T f(t,\sum_{j=0}^{n} y_j\ {}_0I_t^{\alpha}L_j(t;\alpha)+\sum_{i=0}^{k}\frac{x_i}{i!}t^i,\frac{1}{a(t)}(A\sum_{j=0}^{n} y_j\ {}_0I_t^{\alpha-k}L_j(t;\alpha)\\
&+B\sum_{j=0}^{n} y_jL_j(t;\alpha)-g(t,\sum_{j=0}^{n} y_j\ {}_0I_t^{\alpha}L_j(t;\alpha)+\sum_{i=0}^{k}\frac{x_i}{i!}t^i))dt\\
&=\phi(T,\sum_{j=0}^{n} y_j\ {}_0I_T^{\alpha}L_j(t;\alpha)+\sum_{i=0}^{k}\frac{x_i}{i!}T^i)\\
&+\frac{T}{2}\int_{-1}^{1} f(\frac{T}{2}(\tau+1),\sum_{j=0}^{n} y_j\ {}_0I_\tau^{\alpha}L_j(\frac{T}{2}(\tau+1)\alpha)+\sum_{i=0}^{k}\frac{x_i}{i!}(\frac{T}{2}(\tau+1))^i,\\
&\frac{1}{a(\frac{T}{2}(\tau+1))}(A\sum_{j=0}^{n} y_j\ {}_0I_\tau^{\alpha-k}L_j(\frac{T}{2}(\tau+1);\alpha)+B\sum_{j=0}^{n} y_jL_j(\frac{T}{2}(\tau+1);\alpha)\\
&-g(\frac{T}{2}(\tau+1),\sum_{j=0}^{n} y_j\ {}_0I_\tau^{\alpha}L_j(\frac{T}{2}(\tau+1);\alpha)+\sum_{i=0}^{k}\frac{x_i}{i!}(\frac{T}{2}(\tau+1))^i))dt\\
&=\phi(T,\sum_{j=0}^{n} y_j\ {}_0I_T^{\alpha}L_j(t;\alpha)+\sum_{i=0}^{k}\frac{x_i}{i!}T^i)\\
&+\frac{T}{2}\sum_{m=0}^{N}\omega_m f(\frac{T}{2}(\tau_m+1),\sum_{j=0}^{n} y_j\ {}_0I_{\tau_m}^{\alpha}L_j(\frac{T}{2}(\tau_m+1)\alpha)+\sum_{i=0}^{k}\frac{x_i}{i!}(\frac{T}{2}(\tau_m+1))^i,\\
&\frac{1}{a(\frac{T}{2}(\tau_m+1))}(A\sum_{j=0}^{n} y_j\ {}_0I_{\tau_m}^{\alpha-k}L_j(\frac{T}{2}(\tau_m+1);\alpha)+B\sum_{j=0}^{n} y_jL_j(\frac{T}{2}(\tau_m+1);\alpha)\\
&-g(\frac{T}{2}(\tau_m+1),\sum_{j=0}^{n} y_j\ {}_0I_{\tau_m}^{\alpha}L_j(\frac{T}{2}(\tau_m+1);\alpha)+\sum_{i=0}^{k}\frac{x_i}{i!}(\frac{T}{2}(\tau_m))),
\end{aligned}$$

where $t=\frac{T}{2}(\tau+1)$, $\tau\in[-1,1]$ and $\{\tau_m,\omega_m\}_{m=0}^{N}$ be a set of Legendre - Gauss type nodes and weights. In this way, the FOCPs can transform into nonlinear programming (NLP) that we can obtain the necessary conditions, according to differential calculus

$$\frac{\partial J_n(y_0,y_1,\dots,y_n)}{\partial y_j}=0,\qquad j=0,1,\dots,n.$$

The above nonlinear equations can be solved by Newton's iterative or fminsearch in MATLAB and determine the optimization values of y_j to approximate $y(t)$, finally we can approximate the state $x(t)$ and the control $u(t)$ by (20) and (21) respectively.

Remark 4.1. The above approach which restricted to special case of dynamics system, it is also applicable to FOCPs which dynamic constraints are described as

$$Ax^{(k)}(t) + B\,{}_0^cD_t^{\alpha}x(t) = g(t, x(t), u(t)), \qquad k \geq 0,$$

it will be possible by applying the Lagrange multiplier technique.

5. Error Bounds for The Approximate Fractional Operators

In the ensuing text, we present upper bounds for estimating errors. The convergence of pseudospectral methods for IOCPs and FOCPs has been discussed in [7,19,20,29]. Furthermore, in [**?**], efficient implementation procedures for the Müntz-Galerkin method have been developed, accompanied by optimal error estimates.

Let $\Pi_{n,\alpha} : L^2(0,1) \longrightarrow \mathbf{M}_{n,\alpha}$ be the orthogonal projection defined as $(\Pi_{n,\alpha}u - u, v_n) = 0 \qquad v_n \in \mathbf{M}_{n,\alpha}$, where u is an element of $L^2(0,1)$. Following its definition, we have:

$$(\Pi_{n,\alpha})u(x) = u_n(x) = \sum_{k=0}^{n} u_k L_k(t;\alpha),$$

where u_j is given by (10). It can be demonstrated that $(\Pi_{n,\alpha})u(x)$ serves as the best approximation to $u(x)$ within $\mathbf{M}_{n,\alpha}$ (refer to [**?**]). Additionally, we can define the weighted Sobolev space in the interval $(0,1]$:

$$B_{\alpha}^1 = \left\{u \mid u \in L^2, \partial_t u \in L_w^2\right\},$$

equipped with the norm and semi-norm

$$\| u \|_{B_{\alpha}^1} = (\| u \|_{L^2}^2 + \| \partial_t u \|_{L_w^2}^2)^{\frac{1}{2}}, \qquad | u |_{B_{\alpha}^1} = \| \partial_t u \|_{L_w^2}.$$

Theorem 5.1. *Consider $\alpha > 0$ and $w(t) = t^{2-\alpha}(1-t^{\alpha})$. The derivatives of Müntz-Legendre functions, denoted as $\{\partial_t L_n(t;\alpha)\}$, are mutually orthogonal in $L_w^2(0,1)$, and*

$$\int_0^1 w(t)\partial_t L_n(t;\alpha)\partial_t L_m(t;\alpha)dt = \frac{n\alpha(n\alpha+1)}{2n\alpha+1}\delta_{nm}. \tag{22}$$

Proof. By using $\partial_t L_n(t;\alpha) = (n\alpha+1)t^{\alpha-1}P_{n-1}^{1,\frac{1}{\alpha}}(2t^\alpha - 1)$ and orthogonality of Jacobi functions, we have

$$\begin{aligned}
&\int_0^1 w(t)\partial_t L_n(t;\alpha)\partial_t L_m(t;\alpha)dt \\
&\quad = \int_0^1 w(t)(n\alpha+1)t^{\alpha-1}P_{n-1}^{1,\frac{1}{\alpha}}(2t^\alpha - 1)(m\alpha+1)t^{\alpha-1}P_{m-1}^{1,\frac{1}{\alpha}}(2t^\alpha - 1)dt \\
&\quad = (n\alpha+1)(m\alpha+1)\int_0^1 t^\alpha(1-t^\alpha)P_{n-1}^{1,\frac{1}{\alpha}}(2t^\alpha - 1)P_{m-1}^{1,\frac{1}{\alpha}}(2t^\alpha - 1)dt \\
&\quad = \frac{(n\alpha+1)(m\alpha+1)}{\alpha}\int_0^1 (1-\tau)\tau^{\frac{1}{\alpha}}P_{n-1,1}^{1,\frac{1}{\alpha}}(\tau)P_{m-1,1}^{1,\frac{1}{\alpha}}(\tau)d\tau \\
&\quad = \frac{n\alpha(n\alpha+1)}{2n\alpha+1}\delta_{nm},
\end{aligned}$$

where $\tau = t^\alpha$. □

Lemma 5.2. *For $0 < \alpha < 1$ and any $u \in \mathbf{M}_{n,\alpha}$, we have*

$$\|\partial_t u\|_{L^2_w} \leq \sqrt{n\alpha(n\alpha+1)}\|u\|_{L^2}. \tag{23}$$

Proof. For any $u \in \mathbf{M}_{n,\alpha}$, we can write

$$u(t) = \sum_{k=0}^{n} u_k L_k(t;\alpha), \qquad u_k = (2k\alpha+1)\int_0^1 u(t)L_k(t;\alpha)dt. \tag{24}$$

Thus, leveraging the orthogonality of Müntz-Legendre polynomials,

$$\|u\|^2_{L^2} = \sum_{k=0}^{n} \frac{|u_k|^2}{2k\alpha+1}.$$

By differentiating (24) and utilizing (22), we can derive:

$$\begin{aligned}
\|u\|^2_{L^2_w} = \sum_{k=1}^{n}\sum_{j=1}^{n} u_k u_j (\partial_t L_k(t;\alpha), \partial_t L_j(t;\alpha)) &= \sum_{k=1}^{n} \frac{k\alpha(k\alpha+1)}{2k\alpha+1}|u_k|^2 \\
&\leq n\alpha(n\alpha+1)\|u\|^2_{L^2}.
\end{aligned}$$

□

Theorem 5.3. *Let $0 < \alpha < 1$ and ${}_0^cD_t^{k\alpha}u(t) \in \mathbf{C}(0,1]$ for $k = 0, 1, \ldots, n+1$, then the error bound can be represented as follows*

$$\|\Pi_{n,\alpha}u - u\|_{L^2} \leq \frac{\kappa_{\alpha,1}}{\Gamma((n+1)\alpha+1)\sqrt{(2(n+1)\alpha+1)}}, \tag{25}$$

and

$$\|\partial_t(\Pi_{n,\alpha}u - u)\|_{L^2_w} \leq \frac{\kappa_{\alpha,1}\sqrt{n\alpha(n\alpha+1)}}{\Gamma((n+1)\alpha+1)\sqrt{(2(n+1)\alpha+1)}}, \tag{26}$$

where $\kappa_{\alpha,1}$ is a positive constant such that $|{}_0^cD_t^{(n+1)\alpha}u(t)| < \kappa_{\alpha,1}$, $x \in (0,1]$.

Proof. By the definition of the best approximation $\Pi_{n,\alpha}u$, we can write

$$\|\Pi_{n,\alpha}u - u\|_{L^2} \leq \|u - v_n\|_{L^2}, \qquad \forall v_n \in \mathbf{M}_{n,\alpha}.$$

We consider the Generalized Taylors formula $v_n(t) = \sum_{k=0}^{n} \frac{{}_0^cD_t^{k\alpha}u(t)(0)}{\Gamma(k\alpha+1)} t^{k\alpha}$, it is easy to obtain

$$|u(t) - \sum_{k=0}^{n} \frac{{}_0^cD_t^{k\alpha}u(t)(0)}{\Gamma(k\alpha+1)} t^{k\alpha}| \leq \frac{t^{(n+1)\alpha}}{\Gamma((n+1)\alpha+1)} \kappa_{\alpha,1},$$

then

$$\begin{aligned} \| \Pi_{n,\alpha}u - u \|_{L^2}^2 \leq \| \frac{t^{(n+1)\alpha}}{\Gamma((n+1)\alpha+1)} \kappa_{\alpha,1} \|_{L^2}^2 &= \frac{\kappa_{\alpha,1}^2}{\Gamma((n+1)\alpha+1)^2} \int_0^1 t^{2(n+1)\alpha} dt \\ &= \frac{\kappa_{\alpha,1}^2}{\Gamma((n+1)\alpha+1)^2 (2(n+1)\alpha+1)}, \end{aligned}$$

By taking the square roots, the inequality (25) can be obtained. Also, by using Lemma (5.2), we can conclude the second inequality. □

The next Theorem gives the error bounds for left RLFI and left and right CFD are introduced in Section 2.

Theorem 5.4. *Under the conditions of Theorem 5.3,*

$$\begin{aligned} &\| \, {}_0I_t^{\alpha}\Pi_{n,\alpha}u - {}_0I_t^{\alpha}u \, \|_{L^2} \leq \frac{\kappa_{\alpha,1}}{\Gamma(1+\alpha)\Gamma((n+1)\alpha+1)\sqrt{(2(n+1)\alpha+1)}}, \\ &\| \, {}_0^cD_t^{\alpha}\Pi_{n,\alpha}u - {}_0^cD_t^{\alpha}u \, \|_{L^2} \leq \frac{\kappa_{\alpha,2}}{\Gamma(n\alpha+1)\sqrt{(2n\alpha+1)}}, \\ &\| \, {}_t^cD_1^{\alpha}\Pi_{n,\alpha}u - {}_t^cD_1^{\alpha}u \, \|_{L^2} \leq \frac{\kappa_{\alpha,2}}{\Gamma(n\alpha+1)\sqrt{(2n\alpha+1)}}, \end{aligned}$$

where $|{}_0^cD_t^{n\alpha}u(t)| < \kappa_{\alpha,2}, \ x \in (0,1]$.

Proof. For the first inequality, By using the convolution Theorem, we have

$$\| u * v \|_{L^p} \leq \| u \|_1 \| v \|_{L^p} .$$

Then we have the following relations

$$\begin{aligned} \| \, {}_0I_t^{\alpha}\Pi_{n,\alpha}u - {}_0I_t^{\alpha}u \, \|_{L^2} &= \| \frac{1}{\Gamma(\alpha)} \int_0^t (t-s)^{\alpha-1}(u(s) - \Pi_{n,\alpha}u(s))ds \, \|_{L^2} \\ &= \| \frac{1}{\Gamma(\alpha)} t^{\alpha-1} * (u(t) - \Pi_{n,\alpha}u(t)) \, \|_{L^2} \\ &\leq \| \Pi_{n,\alpha}u(t) - u(t) \, \|_{L^2} \frac{1}{\Gamma(\alpha)} \int_0^1 t^{\alpha-1} dt \\ &\leq \frac{\kappa_{\alpha,1}}{\Gamma(1+\alpha)\Gamma((n+1)\alpha+1)\sqrt{(2(n+1)\alpha+1)}} \end{aligned}$$

Since $\Pi_{n,\alpha}\,{}_0^cD_t^\alpha u \in \mathbf{M}_{n-1,\alpha}$, according to Theorem (5.3) , the second inequality can be obtained easily. Finally, one can verify that left and right CFD satisfy ${}_t^cD_1^\alpha u(t) ={}_0^c D_y^\alpha u(y)$, where $y = 1-t$, so we can obtain the last inequality. □

Theorem 5.5. *Let $\{t_i\}_{i=0}^n$ be the collocation points and the conditions of Theorem 5.3, there is a constant $\kappa_{\alpha,3}$ such that*

$$\max_{t\in[t_1,t_{n-1}]} \mid u(t)-\Pi_{n,\alpha}u(t) \mid \leq \kappa_{\alpha,3}\Big(\frac{1+\sqrt{n\alpha(n\alpha+1)}}{\Gamma((n+1)\alpha+1)\sqrt{(2(n+1)\alpha+1)}}\Big)$$

Proof. Let $d = \sqrt{t_{n-1}-t_1}$ and using Gagliardo-Nirenberg interpolation inequality (see appendix B of [**?**]), we have the following inequality

$$\begin{aligned}\max_{t\in[t_1,t_{n-1}]} \mid u(t)-\Pi_{n,\alpha}u(t) \mid &\leq \frac{1}{d} \parallel \Pi_{n,\alpha}u(t)-u(t) \parallel_{L^2(t_1,t_{n-1})} \\ &+ d \parallel \partial_t(\Pi_{n,\alpha}u(t)-u(t)) \parallel_{L^2(t_1,t_{n-1})} \\ &\leq \frac{1}{d} \parallel \Pi_{n,\alpha}u(t)-u(t) \parallel_{L^2(0,1)} + dM_1 \parallel \partial_t(\Pi_{n,\alpha}u(t)-u(t)) \parallel_{L^2_w(0,1)} \\ &\leq \kappa_{\alpha,3}\Big(\frac{1+\sqrt{n\alpha(n\alpha+1)}}{\Gamma((n+1)\alpha+1)\sqrt{(2(n+1)\alpha+1)}}\Big),\end{aligned}$$

where $\kappa_{\alpha,3} = \frac{\kappa_{\alpha,1}\max(1,d^2M_1)}{d}$ and

$$M_1^2 = \max_{x\in[x_1,x_{n-1}]} \frac{1}{t^{2-\alpha}-t^2} = \frac{1}{t_1^{2-\alpha}-t_1^2} = \max\Big(\frac{1}{t_1^{2-\alpha}-t_1^2}, \frac{1}{t_{n-1}^{2-\alpha}-t_{n-1}^2}\Big).$$

□

In the following Theorem, we give the upper bound of the system dynamics for the introduced methods. For this, we define

$$E_{n,\alpha} = x(t) - x_{n,\alpha},$$

where $x_{n,\alpha}$ represents a numerical solution obtained using introduced method.

Theorem 5.6. *Under the conditions of theorem 5.3 and $G(t, x(t), u(t)) = g(t, x(t)) + a(t)u(t)$ as a system dynamics for FOCP introduced in (6) is Lipschitz, with the Lipschitz constant η, then the error bound $E_{n,\alpha}$ for (6) is given by*

$$\parallel E_{n,\alpha} \parallel_{L^2} \leq \frac{2\max(\eta, M_2)\kappa_{\alpha,1}}{\Gamma(1+\alpha)\Gamma((n+1)\alpha+1)\sqrt{2(n+1)\alpha+1}},$$

where $\mid a(t) \mid \leq M_2$.

Proof. Taking the left RLFI of both side of the ${}_0^cD_t^\alpha x(t) = g(t, x(t) + a(t)u(t)$, again by using (25), we can get

$$\begin{aligned}
\| E_{n,\alpha} \|_{L^2} &=\| x(t) + x_0 - \frac{1}{\Gamma(\alpha)} \int_0^t (t-s)^{\alpha-1}(g(s, \Pi_{n,\alpha}x(s)) + a(s)\Pi_{n,\alpha}u(s))ds \|_{L^2} \\
&=\| \frac{1}{\Gamma(\alpha)} \int_0^t (t-s)^{\alpha-1}(g(s, \Pi_{n,\alpha}x(s)) + a(s)\Pi_{n,\alpha}u(s) - g(s, x(s)) - a(s)u(s))ds \|_{L^2} \\
&\leq \frac{1}{\Gamma(\alpha)} \| t^{\alpha-1} \|_1 \| g(t, \Pi_{n,\alpha}x(t)) - g(t, x(t)) + a(t)\Pi_{n,\alpha}u(t) - a(t)u(t) \|_{L2} \\
&\leq \frac{1}{\Gamma(1+\alpha)}(\eta \| x(t) - \Pi_{n,\alpha}x(t) \|_{L^2} + M_2 \| u(t) - \Pi_{n,\alpha}u(t) \|_{L^2}) \\
&\leq \frac{2\max(\eta, M_2)\kappa_{\alpha,1}}{\Gamma(1+\alpha)\Gamma((n+1)\alpha+1)\sqrt{2(n+1)\alpha+1}}
\end{aligned}$$

□

Remark 5.7. It is important to note that we can find upper bound for general system dynamics by imposing some extra conditions.

6. Applications and Numerical Results

In this section, we showcase the capability and efficiency of the introduced approaches. To achieve this goal, we provide several numerical examples for various cases and apply the introduced method to solve them. The MATLAB function *fsolve* is employed for solving the nonlinear systems. In cases where the exact solution $x(t)$ and $u(t)$ are known, the dependence of approximation errors on the discretization parameter n is estimated in the 2-norm, as follows:

$$E_x = \sqrt{\sum_{k=0}^{n}(x_n(t_k) - x(t_k))^2},$$

$$E_u = \sqrt{\sum_{k=0}^{n}(u_n(t_k) - u(t_k))^2},$$

Where $x_n(t)$ and $u_n(t)$ are the obtain solution by using the proposed methods and $x(t)$ and $u(t)$ are the exact solutions. Also, with increasing n, the linear system obtained from methods going to be ill- posed, then we use the proper numerical method to compute the solution of it.

Example 6.1. *(Linear time -invariant problem) Consider the following linear time invariant FOCP in which* $0 < \alpha < 1$. *The problem is to find and optimal*

$(x^*(t), u^*(t))$ *that minimize the cost function [1, 29]*

$$J = \frac{1}{2}\int_0^1 (x^2(t) + u^2(t)),$$
$$s.t. \quad {}_0^cD_t^\alpha x(t) = -x(t) + u(t),$$

and $x(0) = 1$.

For this problem, we have the exact solution in the case of $\alpha = 1$ as follows

$$x(t) = \cosh(\sqrt{2}t) + \rho\sinh(\sqrt{2}t),$$
$$u(t) = (1 + \sqrt{2}\rho)\cosh(\sqrt{2}t) + (\sqrt{2} + \rho)\sinh(\sqrt{2}t),$$

where

$$\rho = -\frac{\cosh(\sqrt{2}) + \sqrt{2}\sinh(\sqrt{2})}{\sqrt{2}\cosh(\sqrt{2}) + \sinh(\sqrt{2})}.$$

We obtain the numerical solutions $x(t)$ and $u(t)$ for various values of α with $n = 4$. The results are depicted in Fig. 4 (right-column). Additionally, Fig. 4 (left-column) displays the state and control variables obtained by [7], where the Jacobi-Gauss points were chosen. It is evident that this choice struggles to approximate these functions near 0 and 1. As α approaches 1, the solutions of the FOCP converge to those of the IOCP. In Fig. 5, numerical results for this problem with $\alpha = 0.8$ obtained by the present method with various values of n at specific points $t \in [0, 1]$ are presented. To provide an overview of the convergence rate, we plot E_x and E_u as functions of the discretization parameter n for our method and the method introduced in [7] in Fig. 6 (right and left, respectively). Their method exhibits semiconvergence; for small n, the method converges and then abruptly starts to diverge. The accuracy and convergence of the method are illustrated by increasing the correct decimal places of the approximations, as shown in Tables 1-2. Furthermore, we obtain the value of the cost function $J = 0.17190925809$ for $\alpha = 0.95$ and $n = 5$.

Example 6.2. *As a second example, we study another FOCP as follows [7]*

$$min \quad J = \int_0^1 ((u(t) - t)^2 + (x(t) - \frac{t^{\alpha+1}}{\Gamma(\alpha+2)} - \frac{t^\alpha}{\Gamma(\alpha+1)})^2 dt,$$
$$s.t \quad {}_0^cD_t^\alpha x(t) = u(t) + 1, \quad x(0) = 0,$$

where the optimal solution to this problem is $(x^*(t), u^*(t)) = (\frac{t^{\alpha+1}}{\Gamma(\alpha+2)} + \frac{t^\alpha}{\Gamma(\alpha+1)}, t)$.

The estimated solutions for various values of α with $n = 3$, and the values of E_x and E_u obtained by our method (on the right) and those introduced in [7](on the left) are illustrated in Figs. 7-8, respectively. Additionally, we demonstrate the increase in the number of correct decimal places of the approximate solutions in Tables 3-4. We achieved a numerical cost function of $J \approx 0$ for any α and $n = 5$.

t	n=10	n=20	n=30	n=40	n=50	n=60
0.1	0.8353	0.835315	0.8353150	0.83531503	0.8353150209	0.83531502094
0.2	0.7169	0.716899	0.7168994	0.71689934	0.7168993372	0.71689933716
0.3	0.6223	0.622255	0.6222551	0.62225507	0.6222550589	0.62225505891
0.4	0.5448	0.544848	0.5448481	0.54484796	0.5448479853	0.54484798531
0.5	0.4809	0.480883	0.4808839	0.48088378	0.4808837974	0.48088379737
0.6	0.4278	0.427807	0.4278064	0.42780634	0.4278063165	0.42780631645
0.7	0.3838	0.383785	0.3837855	0.38378549	0.3837854425	0.38378544253
0.8	0.3475	0.347486	0.3474868	0.34748668	0.3474867443	0.34748674433
0.9	0.3180	0.317968	0.3179673	0.31796720	0.3179671923	0.31796719228
1.0	0.2947	0.294727	0.2947267	0.29472665	0.2947266501	0.29472665009

Table 1. Approximate solution of $x(t)$ for $\alpha = .9$ with different n and t.

t	n=10	n=20	n=30	n=40	n=50	n=60
0.1	0.3832	0.383162	0.38316167	0.383161669	0.3831616693	0.38316166928
0.2	0.3250	0.325054	0.32506167	0.325062908	0.3250627159	0.32506237877
0.3	0.2762	0.276132	0.27613661	0.276135646	0.2761357215	0.27613581172
0.4	0.2336	0.233621	0.23362073	0.233620676	0.2336206707	0.23362067522
0.5	0.1959	0.195857	0.19585738	0.195858209	0.1958577900	0.19585766721
0.6	0.1616	0.161580	0.16157472	0.161576210	0.1615761739	0.16157576659
0.7	0.1297	0.129684	0.12968687	0.129688172	0.1296887841	0.12968908843
0.8	0.0992	0.099171	0.09916668	0.099169693	0.0991707375	0.09917004395
0.9	0.0689	0.068921	0.06890306	0.068908975	0.0689074722	0.06890724399
1.0	0.0374	0.037399	0.03739510	0.037393657	0.0373929201	0.03739249274

Table 2. Approximate solution of $u(t)$ for $\alpha = .9$ with different n and t.

t	n=10	n=20	n=30	n=40	n=50	n=60	Exact
0.1	0.179615	0.1796190	0.17961906	0.179619062	0.1796190634	0.179619063969	0.179619064277
0.2	0.329193	0.3291946	0.32919468	0.329194688	0.3291946890	0.329194689375	0.329194689653
0.3	0.478095	0.4780960	0.47809601	0.478096017	0.4780960181	0.478096018478	0.478096018701
0.4	0.630475	0.6304773	0.63047736	0.630477368	0.6304773690	0.630477369325	0.630477369526
0.5	0.787956	0.7879572	0.78795727	0.787957271	0.7879572719	0.787957272169	0.787957272350
0.6	0.951329	0.9513297	0.95132973	0.951329732	0.9513297331	0.951329733305	0.951329733463
0.7	1.121029	1.1210301	1.12103008	1.121030088	1.1210300884	1.121030088626	1.121030088767
0.8	1.297310	1.2973112	1.29731119	1.297311195	1.2973111959	1.297311196127	1.297311196258
0.9	1.480322	1.4803234	1.48032338	1.480323386	1.4803233865	1.480323386668	1.480323386792
1	1.670154	1.6701553	1.67015531	1.670155314	1.6701553148	1.670155315043	1.670155315159

Table 3. Approximate solution of $x(t)$ for $\alpha = .8$ with different n and t.

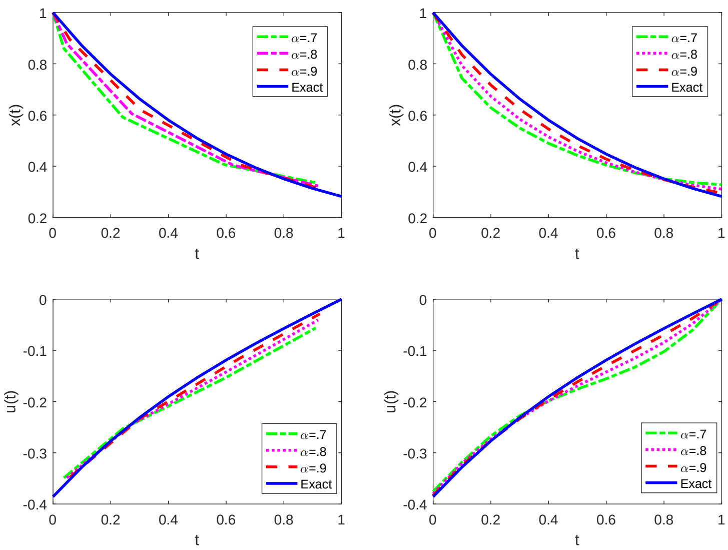

FIGURE 4. Approximate solution of $x(t)$ and $u(t)$ for some α obtained by our method (right-column) and [7] (left-column).

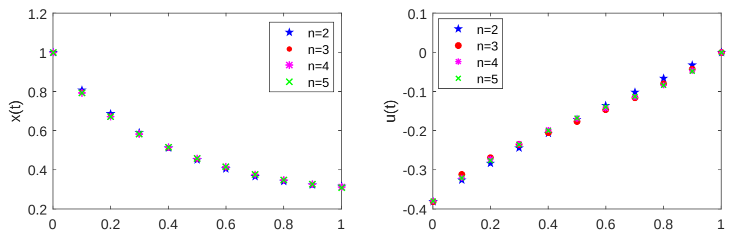

FIGURE 5. The behavior of $x(t)$ and $u(t)$ for $\alpha = .8$ with different values of n.

Example 6.3. *(Nonlinear time -variant problem) We consider the following nonlinear FOCP with fixed final time: Find the control $u^*(t)$ and the state $x^*(t)$ which minimizes the performance index [25]*

$$J = \int_0^1 (tu(t) - (\alpha + 2)x(t))^2 dt,$$

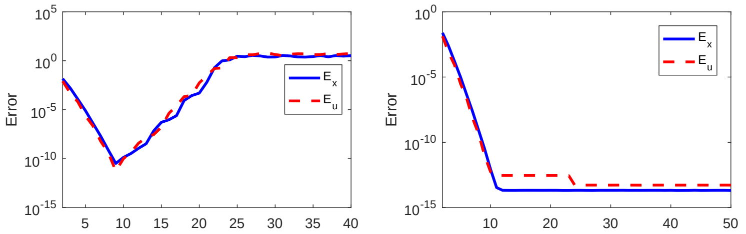

FIGURE 6. The errors E_x and E_u obtained by our method (right) and [7] (left).

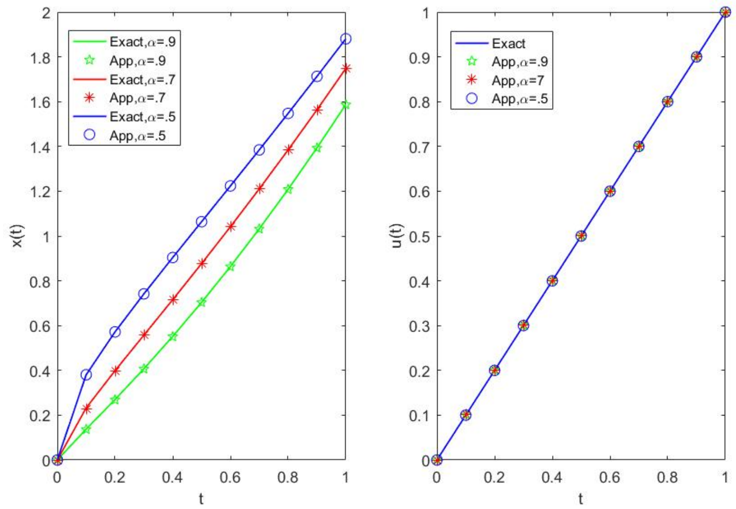

FIGURE 7. Approximate solution of $x(t)$ and $u(t)$ for different values of α.

subject to the dynamic system

$$x'(t) + {}_0^c D_t^\alpha x(t) = u(t) + t^2,$$

and the boundary conditions

$$x(0) = 0, \qquad x(1) = \frac{2}{\Gamma(3+\alpha)}.$$

The solution is given by

$$(x^*(t), u^*(t)) = (\frac{2t^{\alpha+2}}{\Gamma(\alpha+3)}, \frac{2t^{\alpha+1}}{\Gamma(\alpha+2)}).$$

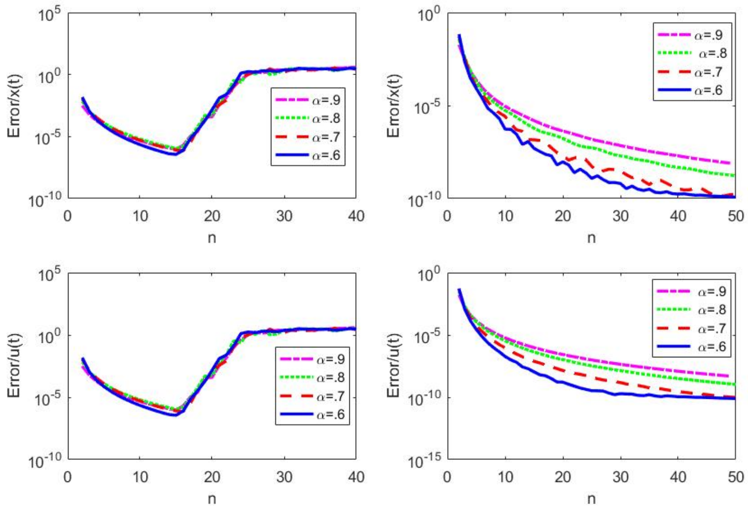

Figure 8. The errors E_x and E_u obtained by our method (right) and [7] (left).

t	n=10	n=20	n=30	n=40	n=50	n=60	Exact
0.1	0.179615	0.1796190	0.17961906	0.179619062	0.1796190634	0.179619063969	0.179619064277
0.2	0.329193	0.3291946	0.32919468	0.329194688	0.3291946890	0.329194689375	0.329194689653
0.3	0.478095	0.4780960	0.47809601	0.478096017	0.4780960181	0.478096018478	0.478096018701
0.4	0.630475	0.6304773	0.63047736	0.630477368	0.6304773690	0.630477369325	0.630477369526
0.5	0.787956	0.7879572	0.78795727	0.787957271	0.7879572719	0.787957272169	0.787957272350
0.6	0.951329	0.9513297	0.95132973	0.951329732	0.9513297331	0.951329733305	0.951329733463
0.7	1.121029	1.1210301	1.12103008	1.121030088	1.1210300884	1.121030088626	1.121030088767
0.8	1.297310	1.2973112	1.29731119	1.297311195	1.2973111959	1.297311196127	1.297311196258
0.9	1.480322	1.4803234	1.48032338	1.480323386	1.4803233865	1.480323386668	1.480323386792
1	1.670154	1.6701553	1.67015531	1.670155314	1.6701553148	1.670155315043	1.670155315159

Table 4. Approximate solution of $u(t)$ for $\alpha = .8$ with different n and t.

The problem is solved for different values of n and α. Fig. 9 shows the exact and approximate state x and the control u as a function of t for $n = 4$ and different values of α. Also in Fig. 10, the numerical solution $x(t)$ and $u(t)$ at $\alpha = .7$ for different values of $n = 2, 3, 4, 5$ are plotted. In this example we take $\alpha = .7$ and the errors E_x and E_u are shown in Fig. 11. In Tables 5-6, we provide the approximated solution for $x(t)$ and $u(t)$ for $\alpha = .8$ and with different values n to show the correct decimal of the approximations. The numerical cost function $J \approx 0$ for any α and $n = 5$ is obtained.

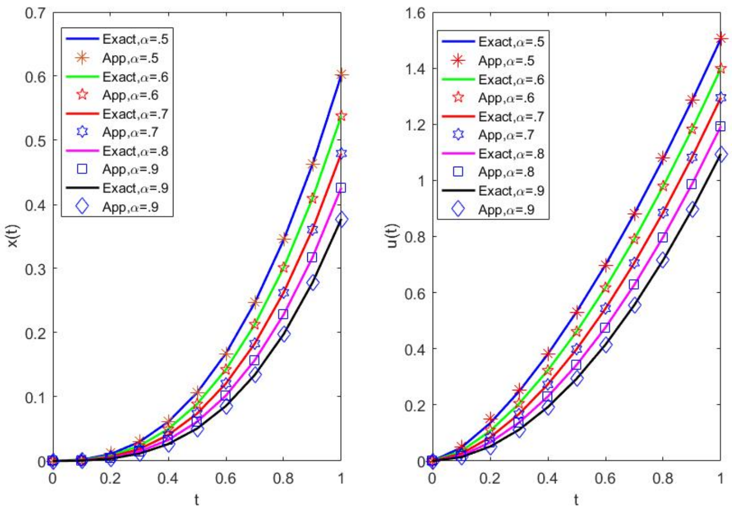

FIGURE 9. Exact and approximation solutions of $x(t)$ and $u(t)$ for different values of α.

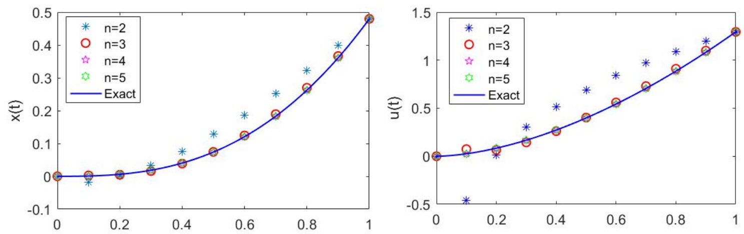

FIGURE 10. The behavior of $x(t)$ and $u(t)$ for $\alpha = .7$ with different values of n.

Example 6.4. *Consider the following nonlinear FOCP [20]*

$$\begin{aligned} &\textit{minimum} \qquad J = \int_0^1 (x(t) - t^2) + (u(t) + t^4 - \frac{20}{9\Gamma(.9)} t^{.9})^2 dt, \\ &{}_0^c D_t^{1.1} x(t) = t^2 x(t) + u(t), \\ &x(0) = x'(0) = 0. \end{aligned}$$

For this problem $x^*(t) = t^2$ and $u^*(t) = \frac{20}{9\Gamma(.9)} t^{.9} - t^4$. This problem has been numerically solved by applying a method which we introduced in section 5. In Fig. 12, the state variable $x(t)$ and the control variable $u(t)$ are plotted

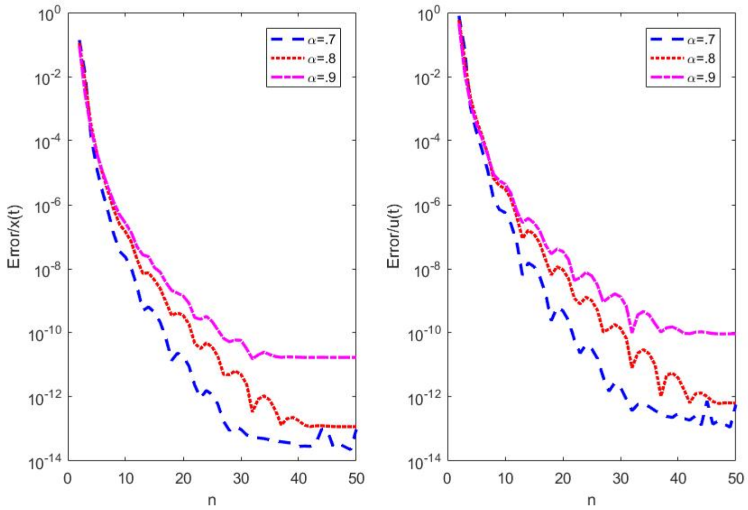

FIGURE 11. The errors E_x and E_u for $\alpha = .7, .8, .9$.

t	n=10	n=20	n=30	n=40	n=50	n=60	Exact
0.1	0.0007	0.000675	0.0006753	0.000675260	0.00067525964	0.0006752596381	0.0006752596401
0.2	0.0047	0.004703	0.0047028	0.004702781	0.00470278127	0.0047027812688	0.0047027812808
0.3	0.0146	0.014636	0.0146356	0.014635592	0.01463559238	0.0146355923842	0.0146355924092
0.4	0.0328	0.032752	0.0327521	0.032752071	0.03275207111	0.0327520711064	0.0327520711442
0.5	0.0612	0.061177	0.0611768	0.061176807	0.06117680681	0.0611768068114	0.0611768068595
0.6	0.1019	0.101928	0.1019282	0.101928186	0.10192818567	0.1019281856743	0.1019281857282
0.7	0.1569	0.156944	0.1569442	0.156944212	0.15694421237	0.1569442123740	0.1569442124274
0.8	0.2281	0.228099	0.2280987	0.228098672	0.22809867182	0.2280986718242	0.2280986718695
0.9	0.3172	0.317212	0.3172122	0.317212154	0.31721215428	0.3172121542846	0.3172121543125

TABLE 5. Approximate solution of $x(t)$ for $\alpha = .8$ with different n and t.

for various of α around 1.1 and $n = 4$. The value $J \approx 0$ for any α and $n = 5$ is obtained for the cost function.

Example 6.5. *Let us consider the following FOCP that minimize [36]*

$$J = \int_0^1 (-2e^{1+t^2+x(t)} + e^{2(1+t^2+x(t))} + 8\sqrt{\frac{t}{\pi}}u(t) - 2u(t)sin(1+t^2)$$
$$+ u^2(t) + 16\frac{t}{\pi} - 8\sqrt{\frac{t}{\pi}}sin(1+t^2) + sin^2(1+t^2) + 1)dt,$$

t	n=10	n=20	n=30	n=40	n=50	n=60	Exact
0.1	0.0189	0.018907	0.01890727	0.0189072699	0.018907269868	0.0189072698678	0.0189072699239
0.2	0.0658	0.065839	0.06583894	0.0658389378	0.065838937763	0.0658389377625	0.0658389379306
0.3	0.1366	0.136599	0.13659886	0.1365988623	0.136598862253	0.1365988622530	0.1365988624861
0.4	0.2293	0.229264	0.22926450	0.2292644977	0.229264497745	0.2292644977448	0.2292644980093
0.5	0.3426	0.342590	0.34259012	0.3425901181	0.342590118144	0.3425901181437	0.3425901184130
0.6	0.4757	0.475665	0.47566487	0.4756648665	0.475664866480	0.4756648664802	0.4756648667316
0.7	0.6278	0.627777	0.62777685	0.6277768495	0.627776849496	0.6277768494958	0.6277768497097
0.8	0.7983	0.798345	0.79834535	0.7983453514	0.798345351385	0.7983453513847	0.7983453515433
0.9	0.9869	0.986882	0.98688226	0.9868822578	0.986882257774	0.9868822577742	0.9868822578611
1	1.1930	1.192968	1.19296808	1.1929680823	1.192968082256	1.1929680822565	1.1929680822565

TABLE 6. Approximate solution of $u(t)$ for $\alpha = .8$ with different n and t.

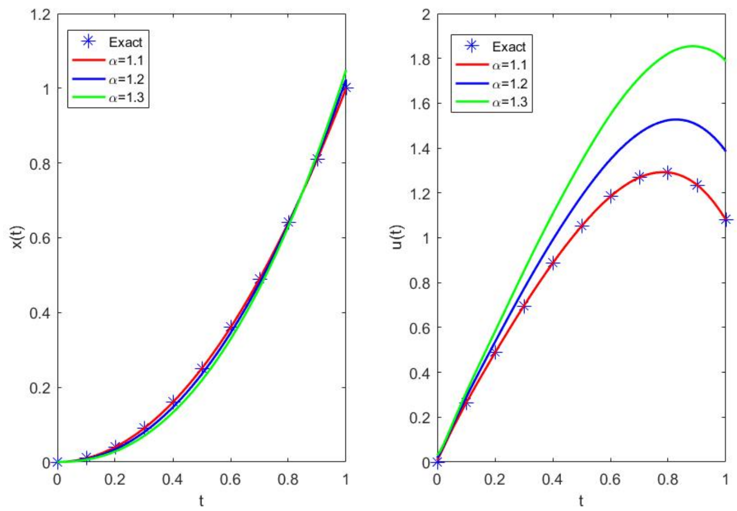

FIGURE 12. Approximate solutions for $n = 5$ and different values of α.

with the given system dynamics and boundary conditions

$$ {}_0^cD_t^{1.5}x(t) = sin(x(t)) + u(t), $$
$$ x(0) = -1 \qquad x'(0) = 0. $$

The exact solution for the pair of control and state functions is

$$ (x^*(t), u^*(t)) = (-t^2 - 1, -4\sqrt{\frac{t}{\pi}} + sin(1 + t^2)). $$

	t								
Example 3	0.1	0.2	0.3	0.4	0.5	0.6	0.7	0.8	0.9
$\lvert x(t) - x_5(t)\rvert$	5.4290E-06	7.8352E-06	1.2947E-05	9.5201E-06	2.5830E-06	8.1553E-06	8.9936E-06	8.5437E-07	4.2936E-06
$\lvert u(t) - u_5(t)\rvert$	8.2349E-04	5.0353E-04	1.9325E-04	1.6647E-04	3.0479E-04	1.6088E-04	1.0695E-04	2.3117E-04	2.9241E-04
Example 4									
$\lvert x(t) - x_5(t)\rvert$	1.0389E-03	9.5331E-05	4.9824E-04	1.1327E-04	5.7843E-04	2.7976E-04	2.0244E-04	6.2062E-05	2.7013E-04
$\lvert u(t) - u_5(t)\rvert$	3.8235E-02	2.7428E-02	1.4848E-03	3.1145E-03	3.5473E-03	2.0499E-04	3.7504E-03	9.6291E-03	4.0514E-02

Table 7. Absolute error of the state and the control functions for Examples 4 and 5

Fig. 13 displays the exact and approximation solution for $x(t)$ and $u(t)$ for $\alpha = 1.5$, $n = 5$ and some others α around 1.5. The value $J \approx 0$ for $\alpha = 1.5$ and $n = 5$ is obtained for the cost function. Also, we can see the absolute error of the state and control functions for some $t \in (0, 1)$ and $n = 4$ in Table 7 for Example 6.4 and 6.5.

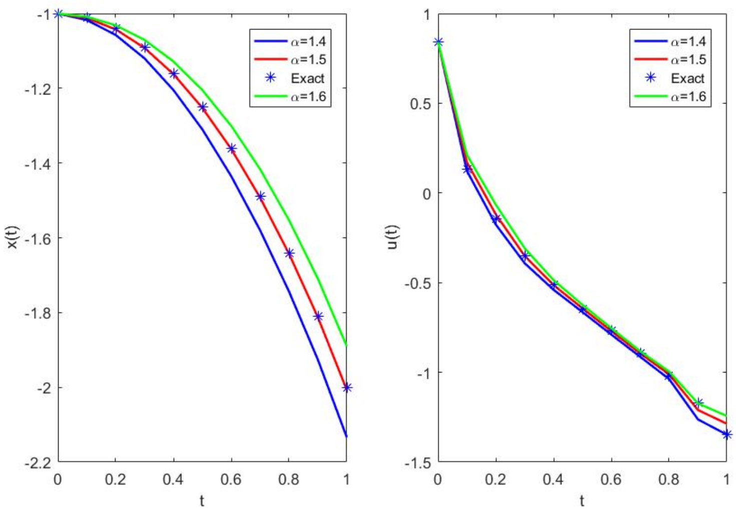

Figure 13. Approximate solutions for $n = 5$ and different values of α.

7. Conclusion

In this paper, we introduced an innovative method called the M*ü*ntz- Legendre In conclusion, this study introduces the innovative method using M*ü*ntz-Legendre polynomials as a promising approach for effectively solving FOCP.

By leveraging the robust properties of M*ü*ntz polynomials, this method aims to achieve both efficiency and stability in the numerical evaluation of fractional operators. Through a comprehensive analysis of error bounds and rigorous convergence analysis, the reliability and convergence properties of the M*ü*ntz-Legendre polynomials have been established. Additionally, numerical examples have been provided to demonstrate the method's effectiveness in solving FOCPs, highlighting its accuracy and computational efficiency. The proposed method contributes significantly to the advancement of numerical techniques for fractional calculus applications, with potential implications across various engineering and scientific domains. Future research could focus on further refining the method and exploring its applicability in more complex systems, thereby expanding its scope and impact in the field.

8. Acknowledgement

The authors are sincerely grateful to the anonymous reviewers for their constructive comments that greatly helped us to improve the paper.

9. Funding

This research received no specific grant from any funding agency in the public, commercial, or not- for-profit sectors.

10. Conflict of interest

The authors declared no potential conflict of interest with respect to the research, authorship, and/or publication of this article.

References

[1] Agrawal, O. P. (2004). *A general formulation and solution scheme for fractional optimal control problems.* Nonlinear Dynamics, 38(1), 323-337.

[2] Agrawal, O. P. (2008). *A formulation and numerical scheme for fractional optimal control problems.* Journal of Vibration and Control, 14(8), 1291-1299.

[3] Almeida, R., Torres, D. F. M. (2011). *Necessary and sufficient conditions for the fractional calculus of variations with Caputo derivatives.* Commun. Nonlinear Sci. Numer. Simul., 16(2011), 1490-1500.

[4] Badalyan, G. V. (1955). *Generalization of Legendre polynomials and some of their applications.* Akad. Nauk Armyan. SSR Izv. Fiz.-Mat. Estest. Tekhn. Nauk, 8, 1-28 and 9 (1956), 3-22 (Russian, Armenian summary).

[5] Borwein, P., Erdélyi, T., Zhang, J. (1994). *Müntz systems and orthogonal Müntz-Legendre polynomials.* Trans. Amer. Math. Soc., 342, 523-542.

[6] Debnath, L. (2003). *Recent applications of fractional calculus to science and engineering.* Int. J. Math. Math. Sci., 54, 3413-3442.

[7] Ejlali, N., Hosseini, S. M. (2017). *A Pseudospectral Method for Fractional Optimal Control Problems.* J. Optim. Theory Appl., 174, 83-107.

[8] Erfani, S., Babolian, E., Javadi, S. (2021). *New fractional pseudospectral methods with accurate convergence rates for fractional differential equations.* Electron. Trans. Numer. Anal., 54, 150-175.

[9] Esmaeili, S., Shamsia, M., Luchko, Y. (2011). *Numerical solution of fractional differential equations with a collocation method based on Müntz polynomials.* Comput. Math. Appl., 62, 918-929.

[10] Garg, D., Patterson, M., Hager, W. W., Rao, A. V., Benson, D. A., Huntington, G. T. (2010). *A unified framework for the numerical solution of optimal control problems using pseudospectral methods.* Automatica, 46, 1843-1851.

[11] Gautschi, W. (1982). *On generating orthogonal polynomials.* SIAM J. SCI. STAT. COMPUT., 3, 289-317.

[12] Heydari, M. H., Hooshmandasl, M. R., Maalek Ghaini, F. M., Cattani, C. (2016). *Wavelets method for solving fractional optimal control problems.* Appl. Math. Comput., 286, 139-154.

[13] Heydari, M. H., Tavakoli, R., Razzaghi, M. (2022). *Application of the extended Chebyshev cardinal wavelets in solving fractional optimal control problems with ABC fractional derivative.* Int. J. Syst. Sci., 53, 2694-2708.

[14] Jarad, F., Abdeljawad, T., Baleanu, D. (2010). *Fractional variational optimal control problems with delayed arguments.* Nonlinear Dyn., 62, 609-614.

[15] Karami, Sh., Fakharzadeh Jahromi, A., Heydari, M. H. (2024). *A cardinal-based numerical method for fractional optimal control problems with Caputo–Katugampola fractional derivative in a large domain.* Int. J. Syst. Sci., 55, 1719-1736.

[16] Ke, X., Chen, Y., Wei, Y. (2015). *Numerical algorithm to solve system of nonlinear fractional differential equations based on wavelets method and the error analysis.* Appl. Math. Comput., 251, 475-488.

[17] Kilbas, A. A., Srivastava, H. M., Trujillo, J. J. (2006). *Theory and Applications of Fractional Differential Equations.* North Holland Mathematics Studies, Elsevier Science B. V., Amsterdam.

[18] Liu, F., Anh, V., Turner, I. (2004). *Numerical solution of the space fractional Fokker-Planck equation.* J. Comput. Appl. Math., 166, 209-219.

[19] Lotfi, A., Dehghan, M., Yousefi, S. A. (2011). *A numerical technique for solving fractional optimal control problems.* Comput. Math. Appl., 62, 1055-1067.

[20] Lotfi, A., Yousefi, S. A., Dehghan, M. (2013). *Numerical solution of a class of fractional optimal control problems via Legendre orthonormal basis combined with the operational matrix and Gauss quadrature rule.* J. Comput. Appl. Math., 250, 143-160.

[21] Maleki, M., Hashim, I., Abbasbandy, S., Alsaedi, A. (2015). *Direct Solution of a Type of Constrained Fractional Variational Problems Via an Adaptive Pseudospectral Method.* J. Comput. Appl. Math., 283, 41-57.

[22] Milovanović, G. V. (1999). *Müntz orthogonal polynomials and their numerical evaluation.* In: Applications and Computation of Orthogonal Polynomials, Internat. Ser. Numer. Math., 131, 179-194.

[23] Mokhtary, P., Ghoreishi, F., Srivastava, H. M. (2016). *The Müntz-Legendre Tau Method for Fractional Differential Equations.* Appl. Math. Model., 40, 671-684.

[24] Podlubny, I. (1998). *Fractional differential equations: an introduction to fractional derivatives, fractional differential equations, to methods of their solution and some of their applications (1st ed.).* San Diego, USA: Academic Press.

[25] Pooseh, S., Almeida, R., Torres, D. F. M. (2014). *Fractional order optimal control problems with free terminal time.* J. Ind. Manag. Optim., 10, 363-381.

[26] Salati, A. B., Shamsi, M., Torres, D. F. M. (2018). *Direct transcription methods based on fractional integral approximation formulas for solving nonlinear fractional optimal control problems.* Commun. Nonlinear Sci. Numer. Simul., doi: 10.1016/j.cnsns.2018.05.011.

[27] Shen, J., Tang, T., Wang, L. L. (2011). *Spectral Methods: Algorithms, Analysis and Applications*, Volume 41 of Series in Computational Mathematics, Springer-Verlag, Berlin, Heidelberg.

[28] Shen, J., Wang, Y. (2016). *Müntz-Galerkin methods and applications to mixed Dirichlet-Neumann boundary value problems.* SIAM J. SCI. COMPUT., 38, 2357-2381.

[29] Tang, X., Liu, Zh., Wang, X. (2015). *Integral fractional pseudospectral methods for solving fractional optimal control problems.* Automatica, 62, 304-311.

[30] Tarasov, V. E. (2011). *Fractional dynamics: applications of fractional calculus to dynamics of particles, fields and media (1st ed.).* Berlin, Germany: Springer-Verlag.

[31] Taslakyan, A. K. (1984). *Some properties of Legendre quasipolynomials with respect to a Müntz system.* Mathematics, Erevan Univ., Erevan, 2, 179-189 (Russian, Armenian summary).

[32] Tohidi, E., Saberi Nik, H. (2015). *A Bessel collocation method for solving fractional optimal control problems.* Appl. Math. Model., 39, 455-465.

[33] Vali, M. A., Valian, F., Ordokhani, Y. (2020). *Numerical solution of fractional optimal control problems with inequality constraint using the fractional-order Bernoulli wavelet functions.* IJST-Trans. Electr. Eng., 44(4), 1513-1528.

[34] West, B. J., Bologna, M., Grigolini, P. (2003). *Physics of Fractal Operators.* Springer-Verlag, NY.

[35] Xu, X., Xiong, L., Zhou, F. (2021). *Solving fractional optimal control problems with inequality constraints by a new kind of Chebyshev wavelets method.* J. Comput. Sci., 54, 101412.

[36] Yousefi, S. A., Nemati, A. (2016). *A numerical method for solving fractional optimal control problems using Ritz method.* J. Comput. Nonlin. Dyn., 11, 051015.

Mohammad Sahabi
Orcid number:
Department of Applied Mathematics
Faculty of Mathematical Sciences
University of Mazandaran
Babolsar, Iran
Email address: mohammadsahabi1368@gmail.com

Allahbakhsh Yazdani Cherati
Orcid number: 0000-0002-3352-5829
Department of Applied Mathematics
Faculty of Mathematical Sciences
University of Mazandaran
Babolsar, Iran
Email address: yazdani@umz.ac.ir